An overview of recent results in finite-temperature lattice QCD

A. Bazavov

Brookhaven National Laboratory

October 16, 2012

Introduction: QGP in theory and experiment

A new state of matter – Quark-Gluon Plasma (QGP) – is expected in QCD due to the asymptotic freedom, and has been observed in heavy-ion collision experiments.

Experiment (RHIC, LHC):

- Particle spectra.
- Heavy-quark bound states.
- Thermal photons and dileptons.

Theory (Lattice QCD):

- Properties of the transition region.
- Fluctuations and correlations of conserved charges.
- The QCD equation of state.
- Correlation functions, spectral functions, transport properties.

Introduction: conjectured phase diagram

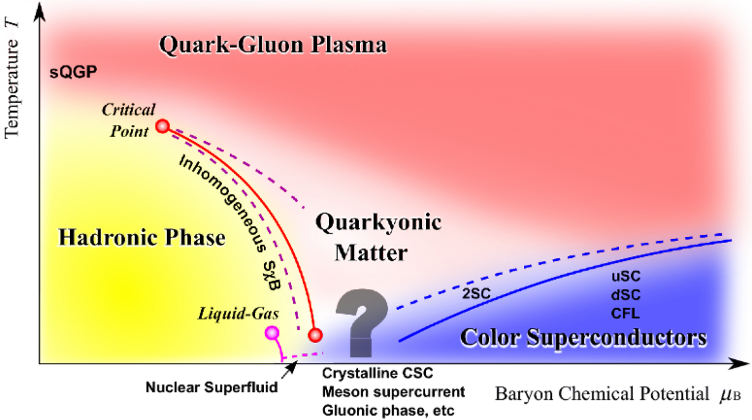

Introduction: Lattice QCD

- Quantum field theory (QCD) in path-integral formulation in Euclidian (imaginary time) formalism:

$$\langle \mathcal{O} \rangle = \frac{1}{Z} \int D\bar{\psi} D\psi DU \; \mathcal{O} \exp(-S),$$

$$Z = \int D\bar{\psi} D\psi DU \exp(-S), \qquad S = \int d^4x \mathcal{L}_E,$$

- Discrete space-time: 4D hypercubic lattice $N_s^3 \times N_\tau$, lattice spacing a serves as a cutoff.
- Temperature is set by compactified temporal dimension: $T = 1/(N_\tau a)$, lattice spacing a is varied at fixed N_τ, or N_τ at fixed a (fixed scale approach).
- Evaluate QCD path integrals stochastically, using Monte Carlo techniques.
- Physics is recovered in the continuum limit (cutoff effects are the major source of systematic uncertainties).

Introduction: Lattice QCD

- Lattice action

$$S = S_{gauge} + S_{fermion}, \qquad S_{fermion} = \sum_{x,y} \bar{\psi}_x M_{x,y} \psi_y$$

  ($M_{x,y}$ is the fermion matrix) preserves the gauge symmetry, but there is the infamous fermion doubling problem – 16 species of fermions in 4D.
- Quarks live on sites and gluons on links as $SU(3)$ matrices

$$U_{x,\mu} = \mathcal{P} \exp \left\{ ig \int_x^{x+a\hat{\mu}} dy_\nu \, A_\nu(y) \right\}.$$

- Fermions are challenging due to the fermion doubling problem and also due to non-locality of the action when the Grasmann variables are integrated out:

$$Z = \int DU \det M[U] \exp(-S_{gauge}).$$

Introduction: Lattice QCD

- Various fermion discretization schemes, at fixed lattice spacing:
  - Staggered – preserve a part of the chiral symmetry, computationally cheap, require taking 4-th root of the Dirac operator.
  - Wilson – no chiral symmetry.
  - Domain-wall – amount of symmetry breaking is controlled by the fifth dimension L_s, exact in $L_s \to \infty$ limit.
  - Overlap – exact chiral symmetry.

Chiral condensate and susceptibility

Chiral condensate:

$$\langle\bar{\psi}\psi\rangle_{q,x} = \frac{1}{4}\frac{1}{N_\sigma^3 N_\tau}\mathrm{Tr}\langle M_q^{-1}\rangle, \quad q = l, s, \quad x = 0, \tau.$$

The susceptibility:

$$\chi_{m,q}(T) \;=\; \frac{\partial\langle\bar{\psi}\psi\rangle_l}{\partial m_q} = 2\chi_{q,disc} + \chi_{q,con}\ ,$$

$$\chi_{q,disc} \;=\; \frac{1}{16 N_\sigma^3 N_\tau}\left\{\langle\left(\mathrm{Tr}M_q^{-1}\right)^2\rangle - \langle\mathrm{Tr}M_q^{-1}\rangle^2\right\}\ ,$$

and

$$\chi_{q,con} \;=\; \frac{1}{4}\mathrm{Tr}\sum_x\langle\, M_q^{-1}(x,0)M_q^{-1}(0,x)\,\rangle\ , \quad q = l, s.$$

The renormalized condensate:

$$\Delta_{l,s}(T) = \frac{\langle\bar{\psi}\psi\rangle_{l,\tau} - \frac{m_l}{m_s}\langle\bar{\psi}\psi\rangle_{s,\tau}}{\langle\bar{\psi}\psi\rangle_{l,0} - \frac{m_l}{m_s}\langle\bar{\psi}\psi\rangle_{s,0}}$$

or

$$\Delta_l^R = d + m_s r_0^4(\langle\bar{\psi}\psi\rangle_{l,\tau} - \langle\bar{\psi}\psi\rangle_{l,0}).$$

Chiral condensate and susceptibility

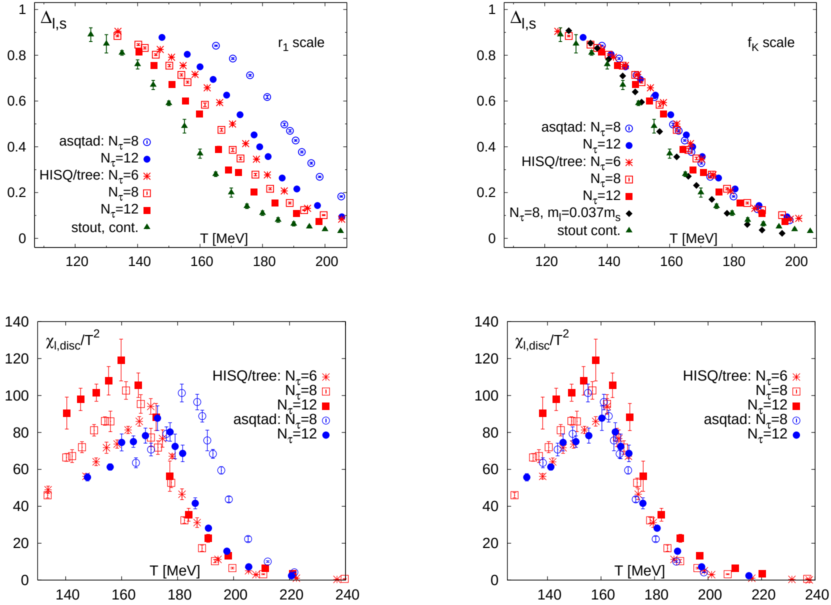

Pseudo-critical temperature, T_c

- At the physical values of light quark masses there is no genuine phase transition in QCD, but a crossover.
- Define a pseudo-transition temperature associated with restoration of chiral symmetry as a peak position in the disconnected chiral susceptibility. (Which diverges in the chiral limit.)
- Agreement on T_c between the groups using staggered fermions, in the continuum limit at the physical light quark masses:
  - BW, stout action, $m_\pi = 140$ MeV, $T_c = 147(4) - 155(4)$ MeV, JHEP09 (2010) 073, arXiv:1005.3508 [hep-lat]
  - HotQCD, HISQ/tree action, $m_\pi = 160$ MeV, extrapolated to $m_\pi = 140$ MeV, $T_c = 154(9)$ MeV, PRD85 (2012) 054503, arXiv:1111.1710 [hep-lat]
- Crosschecks between staggered and other fermion discretization schemes:
  - BW, overlap fermions, $m_\pi = 350$ MeV, arXiv:1204.4089 [hep-lat]
  - BW, Wilson fermions, $m_\pi = 540$ MeV, arXiv:1205.0440 [hep-lat]
  - HotQCD, domain wall fermions, $m_\pi = 200$ MeV, arXiv:1205.3535 [hep-lat]

Chiral symmetry restoration

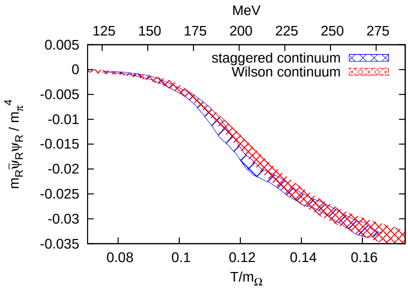

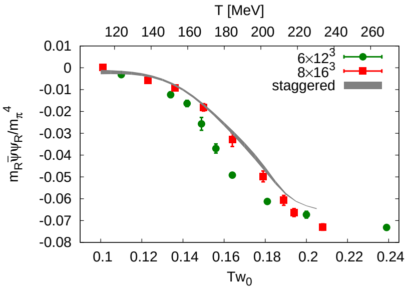

- Left: Renormalized chiral condensate, staggered vs. Wilson.
- Right: Renormalized chiral condensate, staggered vs. overlap.

Chiral symmetry restoration

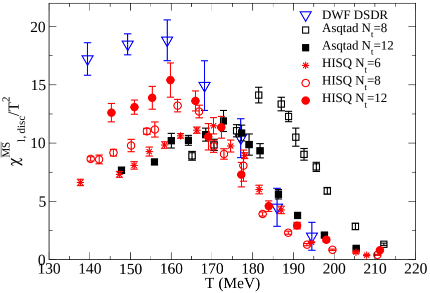

- The disconnected chiral susceptibility, staggered vs. domain wall.
- At fixed lattice spacing, but peak location agrees, difference in height – presumably finite-volume effect.

Chiral symmetry restoration

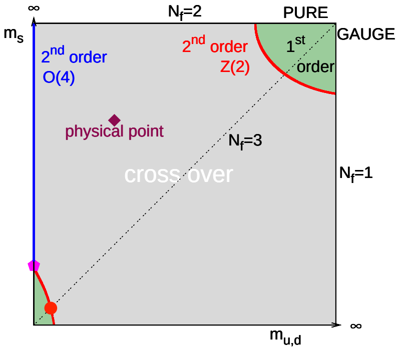

- In the chiral limit the critical behavior is governed by the $O(4)$ universality class.
- At the physical light quark mass scaling behavior with non-universal corrections still applies.
- Search for the first-order region along $m_l = m_s$ line, staggered fermions, Ding et al., arXiv:1111.0185 [hep-lat].
- Current bound on the first-order region $m_\pi = 75$ MeV.

Deconfinement

The Polyakov loop:

$$L_{ren}(T) = z(\beta)^{N_\tau} L_{bare}(\beta), \qquad L_{bare}(\beta) = \left\langle \frac{1}{3} \mathrm{Tr} \prod_{x_0=0}^{N_\tau - 1} U_0(x_0, \vec{x}) \right\rangle$$

- Related to the free energy of a static quark anti-quark pair $L_{ren}(T) = \exp(-F_\infty(T)/(2T))$

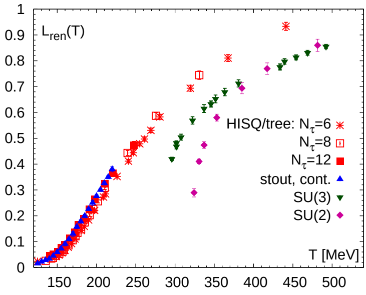

- The increase of $L_{ren}(T)$ (and decrease of $F_\infty(T)$) is related to the onset of screening at higher temperatures.
- The order parameter in pure gauge theory but not in full QCD, the behavior in $SU(2)$, $SU(3)$ and 2+1 flavor QCD is quite different!

Deconfinement

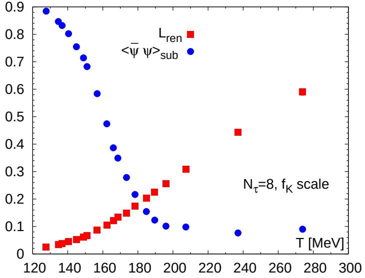

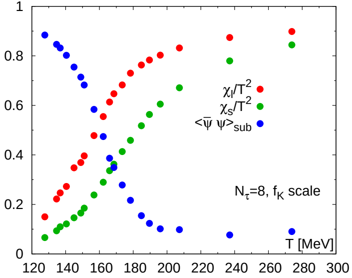

The renormalized chiral condensate plotted together with the renormalized Polyakov loop (left) and the light and strange quark number susceptibility (defined on next slides) (right) for $N_\tau = 8$ lattice, the HISQ/tree action.

Deconfinement happens gradually, no unique transition temperature can be associated with it in full QCD.

Deconfinement: fluctuations

- Fluctuations and correlations of conserved charges:

$$
\begin{aligned}
\frac{\chi_i(T)}{T^2} &= \frac{1}{T^3V}\frac{\partial^2 \ln Z(T,\mu_i)}{\partial(\mu_i/T)^2}\bigg|_{\mu_i=0}, \\
\frac{\chi_{11}^{ij}(T)}{T^2} &= \frac{1}{T^3V}\frac{\partial^2 \ln Z(T,\mu_i,\mu_j)}{\partial(\mu_i/T)\partial(\mu_j/T)}\bigg|_{\mu_i=\mu_j=0}.
\end{aligned}
$$

- Consider light and strange quark number susceptibility.
- At low temperatures they are carried by massive hadrons and their fluctuations are suppressed.
- At high temperatures they are carried by quarks and therefore can signal deconfiment.

Hadron Resonance Gas model

- Following Hagedorn's picture, the Hadron Resonance Gas model approximates the spectrum with currently known states from PDG

$$
\begin{aligned}
p^{HRG}/T^4 &= \frac{1}{VT^3} \sum_{i \in \, mesons} \ln \mathcal{Z}^M_{m_i}(T, V, \mu_{X^a}) \\
&+ \frac{1}{VT^3} \sum_{i \in \, baryons} \ln \mathcal{Z}^B_{m_i}(T, V, \mu_{X^a}),
\end{aligned}
$$

where

$$
\ln \mathcal{Z}^{M/B}_{m_i} = \mp \frac{Vd_i}{2\pi^2} \int_0^\infty dk k^2 \ln(1 \mp z_i e^{-\varepsilon_i/T}) \quad ,
$$

with energies $\varepsilon_i = \sqrt{k^2 + m_i^2}$, degeneracy factors d_i and fugacities

$$
\ln z_i = \sum_a X_i^a \mu_{X^a}/T \ .
$$

Fluctuations: strangeness

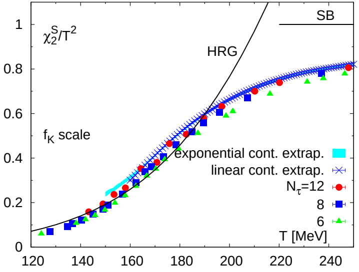

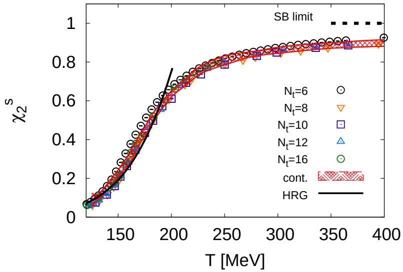

- Left: HotQCD, HISQ/tree action, $m_\pi = 160$ MeV, PRD86 (2012) 034509, arXiv:1203.0784 [hep-lat].
- Right: BW, stout action, $m_\pi = 140$ MeV, JHEP 1201 (2012) 138, arXiv:1112.4416 [hep-lat].

Fluctuations: baryon number

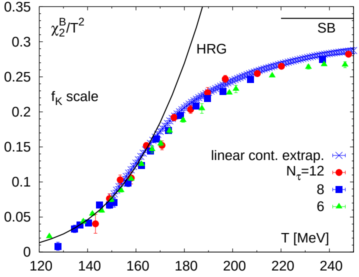

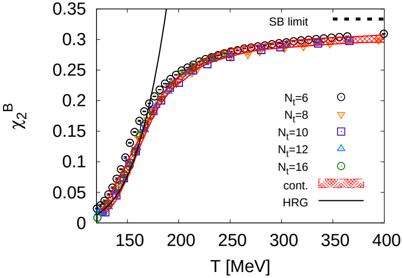

- Left: HotQCD, HISQ/tree action, $m_\pi = 160$ MeV, PRD86 (2012) 034509, arXiv:1203.0784 [hep-lat].
- Right: BW, stout action, $m_\pi = 140$ MeV, JHEP 1201 (2012) 138, arXiv:1112.4416 [hep-lat].

Fluctuations: electric charge

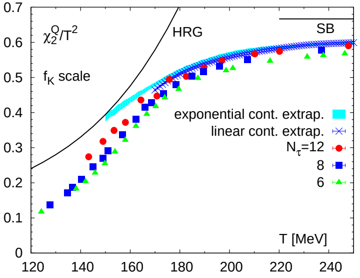

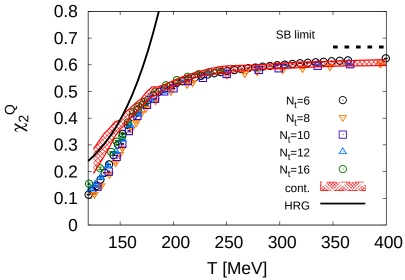

- Left: HotQCD, HISQ/tree action, $m_\pi = 160$ MeV, PRD86 (2012) 034509, arXiv:1203.0784 [hep-lat].
- Right: BW, stout action, $m_\pi = 140$ MeV, JHEP 1201 (2012) 138, arXiv:1112.4416 [hep-lat].

Trace anomaly

- The trace anomaly

$$\varepsilon - 3p = -\frac{T}{V}\frac{d\ln Z}{d\ln a} \quad \Rightarrow \quad \frac{p}{T^4} - \frac{p_0}{T_0^4} = \int_{T_0}^{T} dT' \frac{\varepsilon - 3p}{T'^5}$$

- Requires subtraction of UV divergencies (take difference of zero- and finite-temperature quantities evaluated at the same values of the gauge coupling):

$$\begin{aligned} \frac{\varepsilon - 3p}{T^4} &= R_\beta[\langle S_g\rangle_0 - \langle S_g\rangle_T] \\ &- R_\beta R_m[2m_l(\langle\bar{l}l\rangle_0 - \langle\bar{l}l\rangle_T) + m_s(\langle\bar{s}s\rangle_0 - \langle\bar{s}s\rangle_T)] \end{aligned}$$

$$R_\beta(\beta) = -a\frac{d\beta}{da}, \quad R_m(\beta) = \frac{1}{m}\frac{dm}{d\beta}, \quad \beta = \frac{10}{g^2}$$

Trace anomaly

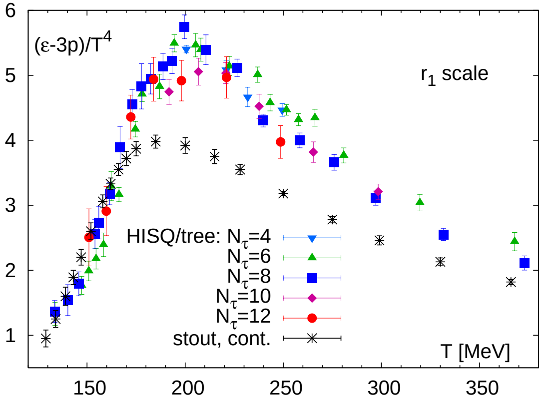

- HotQCD, HISQ/tree action, $m_\pi = 160$ MeV, at fixed N_τ, QM2012, preliminary.
- BW, stout action, $m_\pi = 140$ MeV, JHEP 1011:077,2010, arXiv:1007.2580v2 [hep-lat].
- No agreement so far.

Equation of state

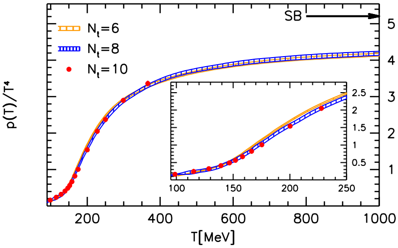

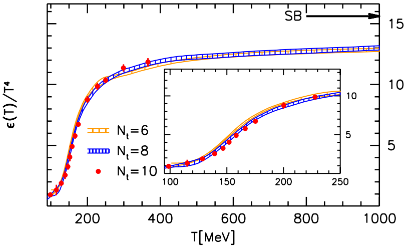

- BW, stout action, $m_\pi = 140$ MeV, JHEP 1011:077,2010, arXiv:1007.2580v2 [hep-lat].
- Pressure (left) and the energy density (right).

Equation of state at $\mu \neq 0$

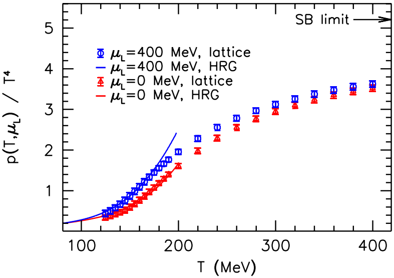

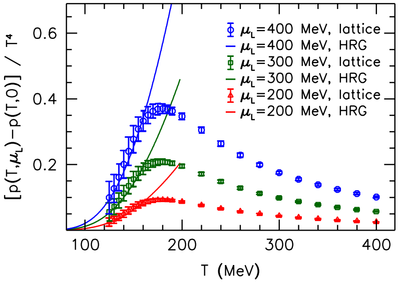

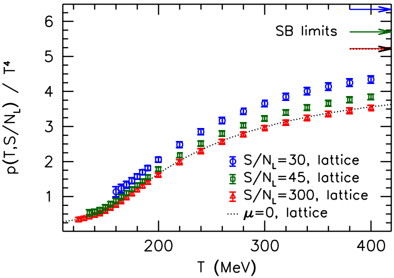

- BW, stout action, $m_\pi = 140$ MeV, arXiv:1204.6710 [hep-lat].
- Pressure (left) and difference from $\mu = 0$ (right).
- Isentropic EoS (bottom).

Heavy quarkonia

The in-medium properties of quarkonium bound states are encoded in spectral functions:

$$\sigma(\omega, \vec{p}, T) = \frac{1}{2\pi} \mathrm{Im} \int dt e^{i\omega t} \int d^3x e^{i\vec{p}\vec{x}} \langle J(\vec{x}, t) J(0,0) \rangle_T$$

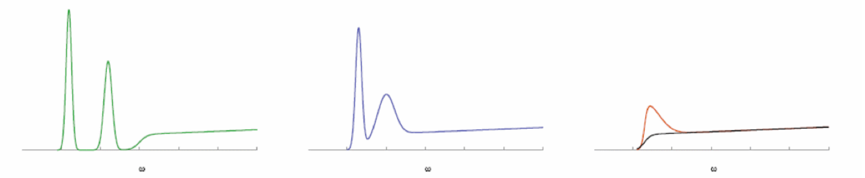

Bound states are represented as sharp peaks in the spectral function. Increase in temperature leads to their broadening and eventual disappearance.
After analytic continuation the spectral function can be related to a quarkonium correlator in Euclidian time:

$$G(\tau, \vec{p}, T) = \int d\omega \sigma(\omega, \vec{p}, T) \frac{\cosh(\omega(\tau - 1/2T))}{\sinh(\omega/2T)}.$$

Heavy quarkonia

Alternatively, one can consider spatial correlation functions:

$$G(z,T) = \int dxdy \int_0^{1/T} d\tau \langle J(x,y,z,\tau) J(0,0,0,0) \rangle,$$

$$G(z,T) = \int_{-\infty}^{\infty} dp_z e^{ip_z z} \int_0^{\infty} d\omega \frac{\sigma(\omega, p_z, T)}{\omega},$$

that also provide information about the temperature dependence of the spectral function.

Existence of a bound state is signaled by a peak in the spectral function, its mass determines the long-distance exponential decay.

At high temperature quark and anti-quark are unbound, therefore the screening mass is given by $2\sqrt{(\pi T)^2 + m_q^2}$.

Heavy quarkonia

The ratio of the pseudo-scalar correlators at finite and zero temperature (left), F. Karsch et al., p4 action, $m_\pi = 220$ MeV, arXiv:1203.3770 [hep-lat].

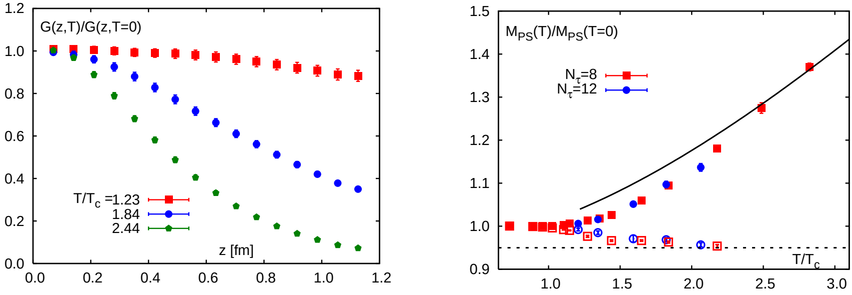

The ratio of the screening masses for periodic and anti-periodic temporal boundary conditions (right).

Thermal photons and dileptons

The vector spectral function in the light quark sector is related to the thermal production rate of dilepton pairs:

$$\frac{\mathrm{d}N_{l^+l^-}}{\mathrm{d}\omega \mathrm{d}^3p} = C_{em} \frac{\alpha_{em}^2}{6\pi^3} \frac{\rho_V(\omega, \vec{p}, T)}{(\omega^2 - \vec{p}^2)(\mathrm{e}^{\omega/T} - 1)}, \qquad C_{em} = \sum_f Q_f^2 .$$

At lightlike 4-momentum it yields the photon emission rate of a thermal medium:

$$\omega \frac{\mathrm{d}R_\gamma}{\mathrm{d}^3p} = C_{em} \frac{\alpha_{em}}{4\pi^2} \frac{\rho_V(\omega = |\vec{p}|, T)}{\mathrm{e}^{\omega/T} - 1},$$

which can be related to the electrical conductivity:

$$\lim_{\omega \to 0} \omega \frac{\mathrm{d}R_\gamma}{\mathrm{d}^3p} = \frac{3}{2\pi^2} \sigma(T) T \alpha_{em} .$$

Thermal photons and dileptons

The vector spectral function has been recently calculated at $1.45\,T_c$ in quenched QCD (H.-T. Ding et al., PRD83 (2011)).

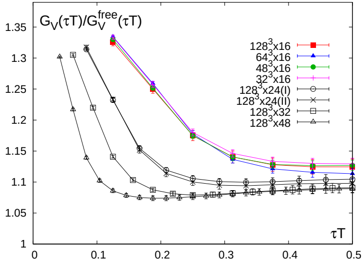

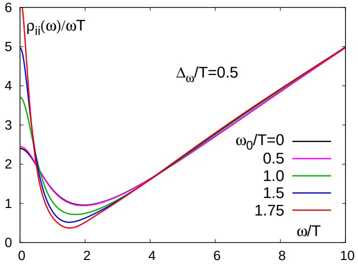

The vector correlation function, $G_V(\tau, T)$ calculated on different lattices (left), and the vector spectral function (right) at different values of the cut-off parameter ω_0.

An estimate for the electrical conductivity

$$1/3 \le \frac{1}{C_{em}}\frac{\sigma}{T} \le 1 \quad \text{at} \quad T \simeq 1.45\ T_c\ .$$

Thermal photons and dileptons

The vector spectral function has been recently calculated at $1.45\,T_c$ in quenched QCD (H.-T. Ding et al., PRD83 (2011)).

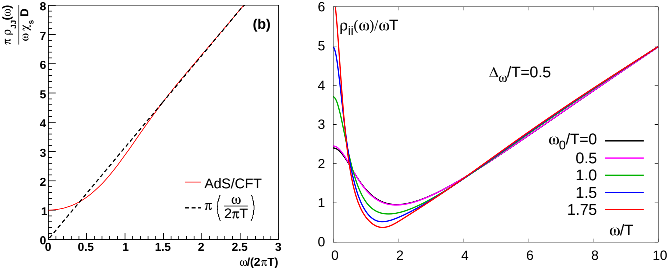

The vector correlation function in $N = 4$ SYM theory[1] (left) and on the lattice (right).

The transport peak at the origin is observed on the lattice and is absent in the strongly-coupled gauge theory.

[1] D. Teaney, PRD74 (2006)

Conclusion

- Pseudo-transition temperature associated with the chiral symmetry restoration is established in the continuum limit at the physical light quark mass. Agreement between staggered studies, crosschecks with Wilson, domain-wall and overlap, but at higher pion mass.
- Deconfinement is a gradual phenomenon, no unique transition temperature can be associated with it in full QCD.
- Fluctuations are useful tools in studying deconfinement, some continuum results are available, agreement between staggered calculations.
- Equation of state: $\sim 20\%$ disagreement, needs more work.
- Interesting results on the behavior of the heavy quark bound states in QGP (and actually many more not discussed in this talk).
- Constraints on the electrical conductivity of QGP in quenched QCD.